JOURNAL OF GEOPHYSICAL RESEARCH, VOL. 113, D15311, doi:10.1029/2008JD009850, 2008

Effects of clouds on ozone profile retrievals from satellite measurements in the ultraviolet

B. van Diedenhoven,[1,2] O. P. Hasekamp,[1] and J. Landgraf[1]

Received 22 January 2008; revised 25 March 2008; accepted 29 April 2008; published 15 August 2008.

[1] We evaluated a new approach to take clouds into account in ozone profile retrievals from backscattered ultraviolet radiance measurements as performed by the Global Ozone Monitoring Experiment (GOME). In this approach ozone profiles are retrieved using cloud fractions, cloud optical thicknesses and top pressures retrieved from oxygen A-band measurements combined with measurements between 350 nm and 390 nm. This approach ($CUVO_2$), is compared with two commonly used approaches in ozone profile retrievals, namely to treat clouds as an effective ground surface albedo (CaA); and using effective cloud fractions and top pressures retrieved from the oxygen A-band by assuming a cloud optical thickness of 40 (Ceff). Using simulated GOME retrievals we show that the CaA and Ceff approaches lead to significant biases in the mean ozone concentrations of up to −85% and 18% near the surface, respectively. With the $CUVO_2$ approach these errors are reduced to below 3%. Retrievals from 233 GOME measurements using the three approaches were validated with ozonesonde measurements at 5 different locations. For most cases the results are as expected from the simulations. For scenes with strong indications for the presence of inhomogeneous clouds, all studied approaches do not correct for cloud sufficiently. The standard deviation of the differences between retrieved profiles and sonde sonde profiles is about 2.5 times larger in the troposphere than expected from the simulations, which indicates that other error sources than clouds dominate the variation in retrieval and/or validation.

Citation: van Diedenhoven, B., O. P. Hasekamp, and J. Landgraf (2008), Effects of clouds on ozone profile retrievals from satellite measurements in the ultraviolet, *J. Geophys. Res.*, *113*, D15311, doi:10.1029/2008JD009850.

1. Introduction

[2] Measurements of the global distribution of vertical ozone profiles are essential to monitor stratospheric and tropospheric ozone concentrations and to study physical and chemical processes in the atmosphere [e.g. *Chandra et al.*, 1999; *Ziemke et al.*, 2005; *de Laat et al.*, 2007]. Such ozone profiles can be retrieved from satellite-based nadir reflectance measurements in the ultraviolet (UV) of sufficient spectral resolution [*Chance et al.*, 1997]. These measurements are provided by the Global Ozone Monitoring Experiment (GOME-1 and GOME-2), the Scanning Imaging Absorption Spectrometer for Atmospheric Chartography (SCIAMACHY) and the Ozone Monitoring Instrument (OMI). For GOME, several algorithms to retrieve ozone profiles are available [*Munro et al.*, 1998; *Hoogen et al.*, 1999; *Hasekamp and Landgraf*, 2001; *van der A et al.*, 2002; *Liu et al.*, 2005]. These algorithms allow ozone profiles to be retrieved from GOME-1 measurements with a Degrees of Freedom for Signal (DFS) of about 4.5–5.5, of which 0.5–1.5 is contributed by the tropospheric layers [*Liu et al.*, 2005].

[3] Since about 98% of the GOME measurements are significantly influenced by clouds [*Krijger et al.*, 2007], ozone profile retrieval algorithms need to accurately take clouds into account, especially to constrain the retrieval errors in the troposphere. However, clouds are generally included in ozone profile retrieval algorithms only in a simplified manner. For example, most algorithms treat clouds as an effective ground surface albedo, thereby ignoring fractional cloud cover and the elevation of clouds. To accurately incorporate clouds into an ozone profile retrieval scheme, the cloud fraction, cloud optical thickness (or albedo) and the cloud top pressure are needed. However, the cloud retrieval algorithms available for GOME generally provide only effective cloud fractions and top pressures, which are here defined as those parameters retrieved under assumption of a fixed cloud optical thickness or a fixed cloud albedo [e.g. *Koelemeijer et al.*, 2001]. The use of these effective cloud parameters in trace gas retrieval schemes can potentially lead to significant errors. For example, for DOAS based tropospheric NO_2 retrievals from GOME measurements it has been shown that the use of effective cloud parameters can lead to a significant systematic overestimation of the tropospheric NO_2 column in the order of 20–50% [*Wang et al.*, 2006; *van Diedenhoven et al.*, 2007]. We therefore introduced a scheme to retrieve

[1] SRON Netherlands Institute for Space Research, Earth Oriented Science Division, Utrecht, Netherlands.
[2] Now at NASA Goddard Institute for Space Studies, New York, New York, USA.

0148-0227/08/2008JD009850$09.00

independent information about cloud fraction, cloud optical thickness and cloud top pressure from GOME measurements at the oxygen A-band and in the UV at 350–390 nm [*van Diedenhoven et al.*, 2007].

[4] In this paper we investigate the effects of clouds on ozone profile retrievals from UV measurements in the spectral range 290–340 nm. Here, we evaluate the suitability of taking clouds into account in ozone profile retrievals by using cloud fraction, cloud optical thickness and cloud top pressure retrieved by the recently developed algorithm by *van Diedenhoven et al.* [2007]. This approach is compared with two commonly used approaches to take clouds into account in ozone profile retrievals, namely: (1) to treat clouds as an effective ground surface albedo; and (2) using effective cloud fraction and top pressure retrieved from measurements at the oxygen A-band assuming a cloud optical thickness of 40.

[5] In section 2 of this paper, the GOME measurements and the ozone profile retrieval approach are discussed. In section 3, the three different approaches to take clouds into account in the ozone profile retrievals are evaluated using simulated measurements. Then, in section 4, ozone profiles are retrieved from real GOME observations using the three different approaches and the results are validated with ozonesonde measurements. We conclude the paper in section 5.

2. GOME Measurements and Retrieval Approach

2.1. GOME Measurements

[6] GOME was launched in 1995 and measures the Earth reflectance in four continuous bands from 237–794 nm, at 0.2–0.4 nm resolution [*Burrows et al.*, 1999]. The instrument scans across track with a swath of 960 km, resulting in near global coverage in three days. For channels 2–4 (312–794 nm), the forward scan is divided into three observations of 320×40 km^2. Furthermore, a backscan of 960×40 km^2 is included in the scan cycle. Because of the large dynamical range in channel 1 (237–312 nm), this channel is split into channel 1a and channel 1b. Measurements of channel 1a (237–307 nm before 6 June 1998, 237–283 nm afterwards) have 960×80 km^2 sized footprints, corresponding to 2 nominal scan cycles. Therefore, we co-add the measurements of channels 1b and 2 to match the channel 1a observations. Thus, the spatial resolution of our retrievals is 960×80 km^2.

[7] In addition to Earth radiance spectra, GOME measures the Solar irradiance. To obtain Earth reflection spectra the Earth radiances are divided by the Solar irradiances. Here, the method of *van Deelen et al.* [2007] is used to account for wavelength shifts between the Earth and Solar spectra due to Doppler or thermally induced shifts between the measurements.

[8] We use version 2.41 of the GOME Data Processor extraction software [*DLR*, 2002], including all standard corrections, e.g. leakage current and stray light. Furthermore, the seasonal dependence of the sun diffuser BSDF is corrected according to *Slijkhuis* [2004]. The polarization correction is not applied since we use vector radiative transfer models to simulate the polarization sensitive measurements. This avoids errors due to an incorrect polarization correction [*Hasekamp et al.*, 2002]. Here, only data from early in the mission (1996–1998) are used to avoid errors due to degradation of the instrument [*van der A et al.*, 2002; *Krijger et al.*, 2005; *Liu et al.*, 2007a].

2.2. Retrieval Approach

2.2.1. Ozone Profile Retrieval

[9] For the retrieval of ozone profiles we use the algorithm of *Hasekamp et al.* [*Hasekamp and Landgraf*, 2001; *Hasekamp et al.*, 2002]. Reflectances and weighting functions for partly cloudy scenes are modeled using the independent pixel approximation [e.g. *Marshak et al.*, 1995]. We employ the vector radiative transfer model of *Hasekamp and Landgraf* [2002] and the CODAGS vector radiative transfer model of *van Diedenhoven et al.* [2006] to describe the radiative transfer in the clear-sky and cloudy part of the atmosphere, respectively. Ozone concentrations at 24 atmospheric layers and the surface albedo are included in the retrieval. Their derivatives are calculated with the forward-adjoint perturbation theory [*Landgraf et al.*, 2001, 2002; *Hasekamp and Landgraf*, 2005]. Measurements in the spectral ranges 290–313 nm and 326–340 nm are used. This wavelength range is extended in comparison to the algorithm of *Hasekamp et al.* [2002], which uses only measurements between 290 and 313 nm. The extension of the wavelength range is expected to increase the sensitivity of the retrievals to tropospheric ozone. Measurements between 313 nm and 326 nm are excluded to avoid the known large calibration errors of the GOME instrument in this wavelength range [*Liu et al.*, 2005]. The ozone absorption cross-sections are taken from *Voigt et al.* [2001]. To account for Ring structures in the GOME data, we include an amplitude and a wavelength shift and squeeze of a precalculated Ring spectrum [*Landgraf et al.*, 2004] in the fit.

[10] The inversion procedure in this algorithm is based on Phillips-Tikhonov regularization [*Phillips*, 1962; *Tikhonov*, 1963] with minimization of the norm of the first derivative with respect to altitude as a side constraint. The regularization parameter is determined by the L-curve technique [*Hansen and O'Leary*, 1993].

[11] Using Phillips-Tikhonov regularization, the retrieval result $\mathbf{x}_{\text{ret}}$ is a smoothed version of the true profile $\mathbf{x}_{\text{true}}$ and is given by

$$\mathbf{x}_{\text{ret}} = \mathbf{A}\mathbf{x}_{\text{true}} + \mathbf{e}_x, \tag{1}$$

where $\mathbf{e}_x$ is the profile error caused by errors in the forward model and measurements, and $\mathbf{A}$ is the averaging kernel matrix [*Rodgers*, 2000]. The DFS of the retrieval is then given by the trace of $\mathbf{A}$ [*Rodgers*, 2000]. For more details about the ozone profile retrieval algorithm, we refer to the paper by *Hasekamp and Landgraf* [2001].

2.2.2. Treatment of Clouds

[12] In this paper, we present ozone profiles retrieved using cloud fractions, cloud optical thickness and cloud top pressures retrieved from measurements at the oxygen A-band and in the UV from 350–390 nm (CUVO_2 approach). The applied cloud retrieval algorithm is described in detail by *van Diedenhoven et al.* [2007]. In brief, cloud fraction, cloud optical thickness and cloud top pressure, in addition to the surface albedos in both wavelength windows and their linear spectral dependence, are simultaneously re-

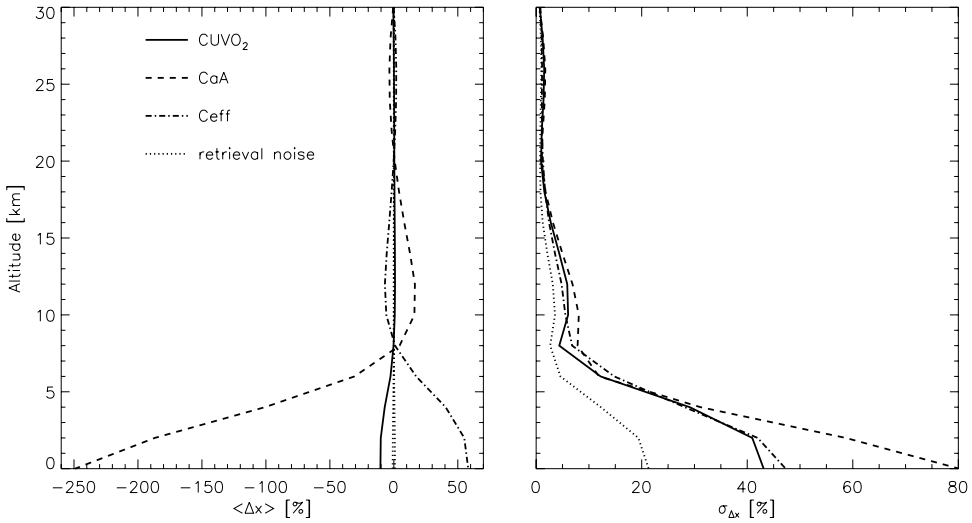

Figure 1. Relative mean differences $\langle \Delta \mathbf{x} \rangle$ (left panel) and their standard deviation $\boldsymbol{\sigma}_{\Delta x}$ (right panel) between ozone profiles retrieved from an ensemble of 200 simulated GOME measurements with randomly chosen cloud parameters and the corresponding smoothed ozone profiles used in the simulated measurements. Here, a noise floor of 0.1% is used. Solid, dashed and dashed-dotted lines correspond to the $CUVO_2$, CaA and Ceff approaches to take into account clouds, respectively. The dotted line indicates the retrieval noise on $\langle \Delta \mathbf{x} \rangle$. The standard deviation of the retrieval noise is determined by the standard deviation of the retrieval results where the correct cloud parameters are used in the retrieval. Here, $\Delta \mathbf{x}$ and $\boldsymbol{\sigma}_{\Delta x}$ are defined relative to the average smoothed input ozone profiles using the $CUVO_2$ averaging kernels.

trieved from these measurements using the Phillips-Tikhonov regularization method. In general, the regularization of the measurement inversion causes a dependence of the retrieval results on a priori information on cloud and surface parameters. However, in our case the retrieved cloud parameters depend only minimally on a priori cloud information for most cloud fractions, but still show a significant dependence on the a priori surface albedos. Thus, the errors in the retrieved cloud parameters are dominated by errors on the a priori surface albedos. The retrieved cloud parameters compare well with those obtained by the Along Track Scanning Radiometer 2 (ATSR-2), which is on the same platform as GOME and has a swath that overlaps with part of the GOME measurements. For cases with inhomogeneous cloud layers, however, the cloud optical thickness is significantly overestimated, while the cloud fraction is underestimated.

[13] The $CUVO_2$ approach is compared with two commonly used approaches to take clouds into account in ozone profile retrievals. In the first alternative approach an effective ground surface albedo is retrieved to account for the enhanced reflection due to the presence of clouds (cloud as albedo (CaA) approach). This approach is used by e.g. *Munro et al.* [1998]; *Hoogen et al.* [1999]; *Hasekamp and Landgraf* [2001]; *van der A et al.* [2002]. The fractional coverage and the elevation of clouds are ignored in this approach. In the second approach, effective cloud fractions and cloud top pressures are used to account for clouds (Ceff approach). This approach is used by e.g. *Liu et al.* [2005] and in the current version of the ozone profile retrieval algorithm (OPERA) developed by the Royal Netherlands Meteorological Institute (KNMI) [see e.g. the overview paper by *Meijer et al.*, 2006]. Effective cloud parameters are those parameters retrieved when assuming a fixed cloud optical thickness (or reflection) [e.g. *Koelemeijer et al.*, 2001]. In this study we retrieve effective cloud fractions and cloud top pressures from measurements at the oxygen A-band, assuming a cloud optical thickness of 40. Such a high cloud optical thickness (or a corresponding cloud albedo of about 0.8) is commonly assumed in algorithms for effective cloud parameters [*Koelemeijer et al.*, 2001; *Liu et al.*, 2005]. *Koelemeijer and Stammes* [1999] and *Wang et al.* [2006] have shown that a cloud albedo of 0.8 is an optimal choice for the retrieval of respectively total ozone columns and tropospheric NO_2 columns. Furthermore, since cloud optical thicknesses above 40 are rare, assuming a cloud optical thickness of 40 limits the possibility of retrieving effective cloud fractions exceeding 1 [*Koelemeijer et al.*, 2001]. (Note that for the rare cases with effective cloud fractions exceeding 1, commonly the fraction is set to 1 and an effective cloud optical thickness (or effective cloud albedo) is retrieved.) In this approach, the surface albedo at the oxygen A-band is assumed a priori since no surface albedo information can be retrieved from the oxygen A-band measurements in combination with the effective cloud fraction and top pressure [*van Diedenhoven et al.*, 2007].

3. Effects of Clouds on Ozone Profile Retrievals Using Simulated Measurements

[14] In this section, the $CUVO_2$, CaA and Ceff approaches to take clouds into account in the ozone profile retrieval are evaluated using simulated measurements. To study the errors on retrieved ozone profiles due to these approaches, GOME measurements are simulated for an

ensemble of 200 scenarios with randomly chosen cloud fractions between 0 and 1 and cloud top pressures between 400 hPa and 800 hPa. Furthermore, a difference between the cloud top and bottom of 200 hPa is assumed. The cloud optical thickness values are randomly chosen from a Gaussian distributed set with a median of 8, a standard deviation of 15 and a minimum cloud optical thickness of 2. This distribution roughly resembles global mean distributions of cloud optical thickness for water clouds, such as observed by e.g., *Rossow and Lacis* [1990] and *Chang and Li* [2005]. A mean surface albedo corresponding to a vegetation surface is used, i.e 0.01 between 290 and 340 nm, 0.05 between 350 and 390 nm and 0.3 at the oxygen A-band around 760 nm. In the ensemble, random variations of ±10% are introduced around the mean surfaces albedos. Then, ozone profiles are retrieved from these simulated measurements using the CaA, Ceff and $CUVO_2$ approaches to account for clouds.

[15] For the $CUVO_2$ approach, an a priori cloud optical thickness of 5 and an a priori cloud top pressure of 500 hPa are taken. For the a priori cloud fraction, the effective cloud fraction that corresponds to the a priori cloud optical thickness of 5 is taken, with a maximum of 1. The mean vegetation surface albedos are used as the a priori surface albedos in the cloud parameter retrievals. All simulations are performed for a nadir viewing geometry with a solar zenith angle of 40°. The atmospheric temperature and pressure profiles are taken from the US standard atmosphere. A single ozone profile is used for all simulations which is obtained by averaging all ozonesonde measurements above Payerne, Switzerland, in the years 1996 and 1997, available from the World Ozone and Ultraviolet Radiation Data Centre (WOUDC, http://www.woudc.org). The GOME noise error is modelled using the instrument noise model described by *Landgraf and Hasekamp* [2007]. Additionally, a noise floor is added to account for other random-like errors, such as forward model errors. Results for two different noise floor values are discussed below.

3.1. Ensemble Simulations

[16] For a noise floor of 0.1%, Figure 1 shows the relative mean differences $\langle \Delta \mathbf{x} \rangle$ between the ozone profiles retrieved with the $CUVO_2$, CaA and Ceff approaches and the input profile used in the simulated measurements which is smoothed by convolution with the corresponding averaging kernels. Relative results are obtained through division by the average smoothed input ozone profiles using the $CUVO_2$ averaging kernels.

[17] In total 233 retrieved ozone profiles are evaluated. Cases in which the cloud retrieval algorithm of the $CUVO_2$ approach did not converge are excluded. This non-convergence is due to non-linear fitting effects and occurs in about 10% of the retrievals with the current version of the algorithm [*van Diedenhoven et al.*, 2007]. The effective cloud parameter retrievals converge in all cases. Also we exclude cases for which the peak-to-peak variability of the total ozone columns, retrieved by the TOGOMI algorithm [*Valks and van Oss*, 2003], in the 6 sub-pixels within the large GOME ground footprints used here (excluding back-scans) exceeds 15 DU. In these cases, the ozonesonde measurement is probably not representative for the large ground scene observed by GOME.

[18] The average DFS of the retrieved ozone profiles is 4.8. In this paper results are evaluated for the altitudes 0–30 km, of which the layers between 0–10 km contribute on average 0.8 to the total DFS and layers between 10–30 km contribute 1.8 to the total DFS. The DFS of these retrievals is about 5.8. The use of the CaA approach leads to a large underestimation of the mean ozone concentrations below 10 km of up to 220% near the surface. Furthermore, an overestimation of up to 16% between 10–20 km is obtained. Similar results are obtained with CaA approach for other solar zenith angles below 70. These errors are due to the neglect of the fractional cloud cover and the elevation of clouds in the CaA approach. The Ceff approach significantly improves on this. However, still an overestimation of the ozone mean concentrations below 10 km of up to 60% is obtained. Furthermore, between 10–20 km an underestimation up to 7% is obtained. The errors due to the Ceff approach slightly decrease with decreasing solar zenith angle between 40° and 70°. These errors are due to the fact that the effective cloud fraction is a wavelength dependent quantity [*van Diedenhoven et al.*, 2007]. This wavelength dependency is caused by the different contributions of the clear-sky part of the observation at different wavelengths due to varying atmospheric scattering and absorption optical thickness and the wavelength dependent surface albedo. Due to the strong increase in contribution of Rayleigh scattered light and increasing ozone absorption cross-sections towards shorter wavelengths, the wavelength dependency of the effective cloud parameters is even observed within the relatively small wavelength window which is used for the ozone profile retrieval, i.e. 290–340 nm. For example, for a fully cloud covered case with a cloud optical thickness of 10 and a cloud top height of 500 hPa, the effective cloud fraction assuming a cloud optical thickness of 40 is 0.59 at 300 nm but 0.53 at 330 nm. Thus, no single value for the effective cloud fraction in the 290–340 nm wavelength range exists. Furthermore, the effective cloud fraction retrieved at the oxygen A-band is relatively high at 0.60. However, also using an effective cloud fraction of 0.56 as retrieved from measurements around 370 nm instead of at the oxygen A-band, as proposed by *Liu et al.* [2005], lead to similar results as shown here. As shown in Figure 1 these errors can be largely avoided by using the $CUVO_2$ approach, which results in errors in the mean tropospheric ozone concentration below 11%. Furthermore, above 10 km the errors are below 1%. For other solar zenith angles, similar results are obtained. These errors are relatively small because in the $CUVO_2$ approach information on both cloud fraction and cloud optical thickness is retrieved, in addition to cloud top pressure. The remaining error is caused by the regularization errors in the cloud parameters due to errors in the a priori cloud and surface parameters.

[19] Figure 1 also shows the standard deviation $\boldsymbol{\sigma}_{\Delta x}$ of $\Delta \mathbf{x}$. For altitudes higher than 10 km, $\boldsymbol{\sigma}_{\Delta x}$ is below 5% for the Ceff and $CUVO_2$ approaches, and somewhat higher (<10%) for the CaA approach. Below about 8 km, the standard deviations strongly increase and are significantly larger than the standard deviation due to the retrieval noise, for all approaches. For the $CUVO_2$ approach $\boldsymbol{\sigma}_{\Delta x}$ is 42% near the surface, of which only 22% is caused by the retrieval noise. Apparently, random errors in the cloud parameters due to errors in the a priori surface albedos lead

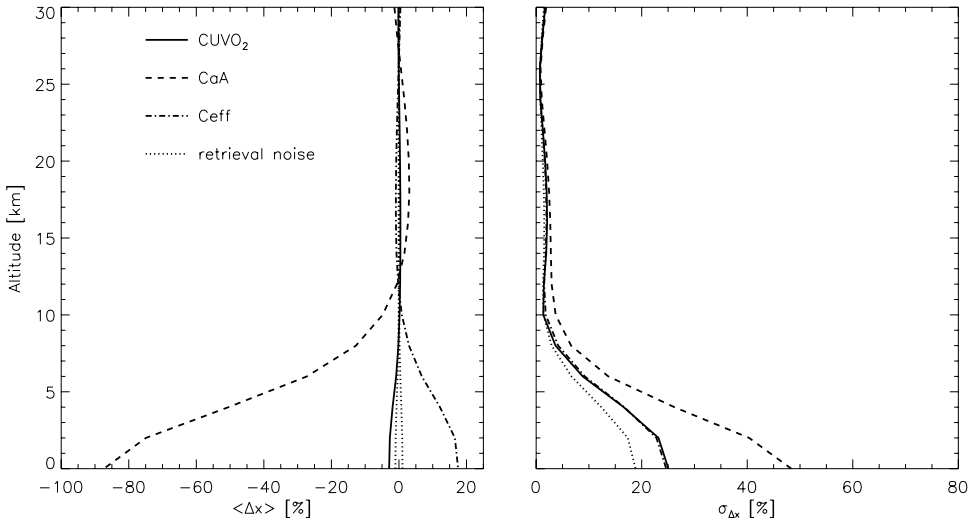

Figure 2. Similar to Figure 1, but for a noise floor of 0.8%.

to an additional error in the retrieved tropospheric ozone concentration.

[20] The influences of clouds on the ozone profile retrievals decrease with decreasing contribution of the tropospheric layers to the DFS. In turn, the DFS decreases with increasing measurement and forward model error, and so does the tropospheric contribution to the DFS. The spectral fitting residuals observed in real GOME retrievals are about 0.8% on average, which is much larger than the measurements noise. The reason for the spectral residuals can be manifold, e.g. errors in the forward model due to insufficient correction of the Ring effect and the 'undersampling' effect [*Chance et al.*, 2005; *van Deelen et al.*, 2007], errors in the ozone cross sections [*Orphal*, 2003; *Liu et al.*, 2007b] or calibration errors of the GOME measurements [*van der A et al.*, 2002; *Liu et al.*, 2005; *Krijger et al.*, 2005]. In the following measurement simulations we account for these errors by adding a noise floor of 0.8%, which leads to an average DFS of about 4.7.

[21] Figure 2 shows $\langle \Delta \mathbf{x} \rangle$ and $\boldsymbol{\sigma}_{\Delta x}$ for a noise floor of 0.8%. The stronger regularization of the inversion results in a significantly smaller effect of clouds compared to the situation shown in Figure 1. The mean ozone concentration is underestimated by up to 85% near the surface when using the CaA approach. The errors in the stratosphere are below 3%. The Ceff approach leads to an overestimation of up to 18% near the surface and below 1% in the stratosphere. Thus, still significant biases are obtained in the troposphere due to the CaA and Ceff approaches. In contrast, the $CUVO_2$ approach leads to errors below 3% in the troposphere, and below 0.5% elsewhere. Also the part of the standard deviations $\boldsymbol{\sigma}_{\Delta x}$ caused by cloud treatment is decreased with the increased noise floor. For the CaA approach, $\boldsymbol{\sigma}_{\Delta x}$ is now 50% at ground level. For the Ceff and $CUVO_2$ approaches, standard deviations of up to about 25% are obtained, which is similar to the standard deviation of the retrieval noise.

3.2. Dependence of Errors on Cloud Parameters

[22] For the CaA and Ceff approaches, the obtained errors systematically depend on the cloud fraction and cloud optical thickness. Additionally, the errors due to the CaA approach depend on cloud top height. The errors due to the $CUVO_2$ approach do not significantly depend on cloud parameters since these are all independently retrieved in this approach. To study how the errors due to the CaA and Ceff approaches depend on cloud fraction, GOME measurements are simulated for a cloud optical thickness of 10 and a cloud top height of 5.6 km (500 hPa) and varying cloud fractions. Here, a noise floor of 0.8% is used. To minimize the effect of retrieval noise, results of 100 cases with different random measurements errors are averaged. Figure 3a shows the error Δx_5 in ozone concentration at a height of 5 km due to the CaA and Ceff approaches as a function of cloud fraction. Already for low cloud fractions of 0.1, the CaA approach leads to significant errors of about -25%. For increasing cloud fraction up to 0.6 the errors due to the CaA approach increase to about -70%. For cloud fractions larger than 0.6 the error slightly decreases. This is because the error due to neglect of fractional cloud cover decreases with increasing cloud fraction, while the error due to the neglect of the cloud elevation remains. For the Ceff approach, Δx_5 is 5% for cloud fractions of 0.1 and increases with cloud fraction to around 30% at a cloud fraction of 1.

[23] Similarly, Figure 3b shows the dependence of Δx_5 on the cloud optical thickness. Here, a cloud fraction of 0.5 and a cloud height of 5.6 km are used. The error due to the CaA approach increases with increasing cloud optical thickness, from about -50% at an optical thickness of 5 to about -85% at an optical thickness of 50. The error due to the Ceff approach is negative for cloud optical thicknesses τ_c lower than 3 and higher than 40 and positive for $3 < \tau_c < 40$. A maximum error of about 20% occurs at cloud optical thickness of 10. This is because of two competing effects that take place with increasing cloud fraction. On the one hand the influence of the cloud on the measurements increases, while on the other hand the effective cloud fraction approaches the geometrical cloud fraction. This leads to a decrease of Δx_5 with increasing cloud optical thickness from 10 up to 40. For a cloud optical thickness of 40 the effective cloud fraction is equal to the geometrical

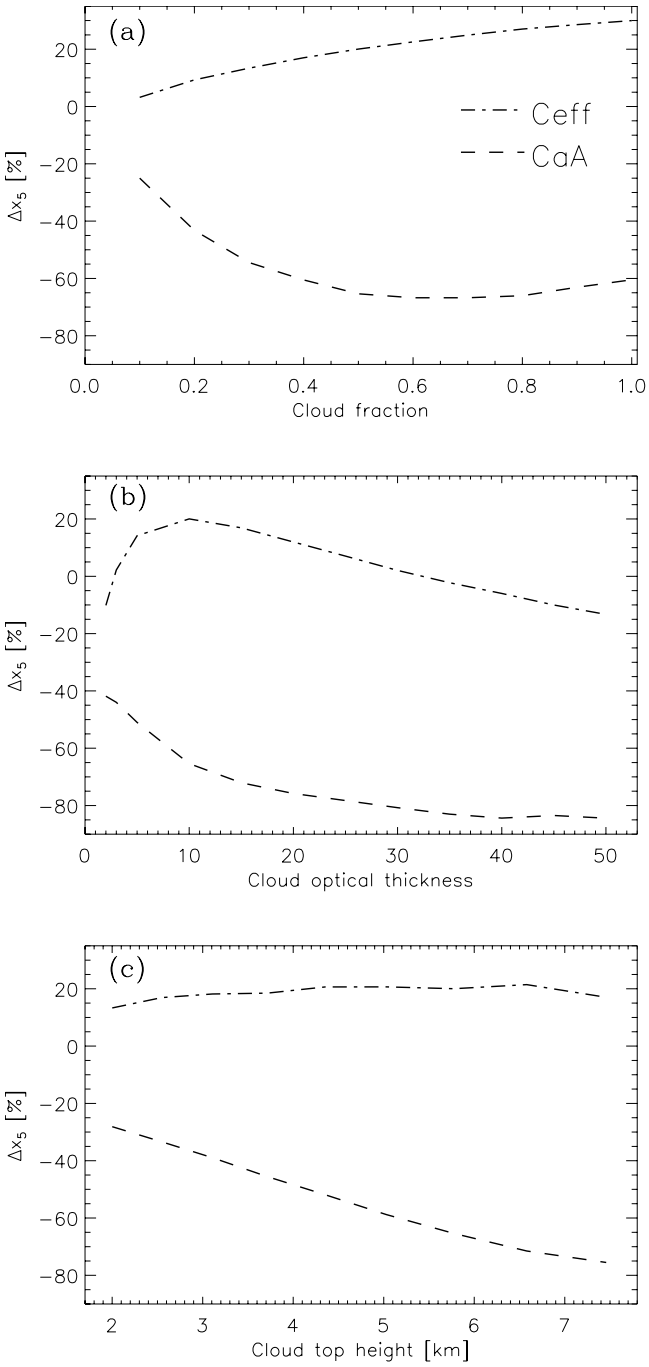

Figure 3. Errors Δx_5 in ozone concentration at 5 km altitude due to the CaA (dashed lines) and Ceff (dashed-dotted lines) approaches as a function of cloud fraction (a), cloud optical thickness (b) and cloud top height (c). The default cloud fraction is 0.5; the default cloud optical thickness is 10; and the default cloud height is 5.6 km. Here, a noise floor of 0.8% is used.

cloud fraction and thus $\Delta x_5 = 0$. For optically thicker clouds the error increases again with reversed sign.

[24] Figure 3c shows Δx_5 as a function of cloud top height. Here, a cloud fraction of 0.5 and a cloud optical thickness of 10 are used. The error due to the CaA approach increases with increasing cloud top height. This is due to the neglect of elevation of clouds in the CaA approach. For the Ceff approach, Δx_5 does not vary significantly with cloud top height. This is because the Ceff approach adequately accounts for the cloud elevation.

3.3. Effect of Aerosols

[25] In addition to clouds, ozone profile retrievals are also affected by the neglect of aerosols in the retrieval [*Liu et al.*, 2005; *van Oss et al.*, 2002]. Furthermore, also biases can be introduced in the retrieved cloud parameters by neglecting aerosols. To study the effect of neglecting aerosols in the retrievals, measurements are simulated for an atmosphere including biomass-burning type aerosols with a total optical thickness of 0.3 at 550 nm in the bottom kilometer of the atmosphere. Note that the aerosols are always below the level of cloud base in these simulations. Subsequently, cloud parameters and ozone profiles are retrieved assuming an atmosphere without aerosols.

[26] Figure 4 shows the effect of neglecting aerosols on the ozone profile retrieval results using the $CUVO_2$, Ceff and CaA approaches as a function of cloud fraction. Compared to the errors in clean atmospheres as shown in Figure 3a, the errors due to the CaA approach are reduced by about 15–25% due to compensating errors. When using the $CUVO_2$ and Ceff approaches, for moderate cloud fractions neglecting aerosols gives a (additional) positive bias of about 15% which is reduced to about 5% for high cloud fractions. The errors only slightly increase for increasing aerosol optical thicknesses between 0.1 and 0.5. For aerosol optical thicknesses lower than 0.1, the errors sharply decrease with decreasing aerosol optical thickness. For increasing cloud optical thickness the effect of aerosols decreases since the relative effect of aerosols on the radiances decreases. Furthermore, less light is penetrating through optical thicker clouds towards the aerosol layer.

3.4. Impact of Clouds on Averaging Kernels

[27] To demonstrate the effect of clouds on the averaging kernels of the retrieved ozone profiles we compare retrievals from simulated measurements of a clear-sky case and a cloudy case. Here, a noise floor of 0.8% is used. In the cloudy case, a cloud is present with a optical thickness of 10, a top-height of 5 km (520 hPa) and a base-height of 2.8 km (720 hPa). Figure 5 shows the averaging kernels for the clear-sky case and for the cloudy case using the CaA and $CUVO_2$ approach. For the clear-sky case, the tropospheric averaging kernels are relatively broad and all peak at a height of about 7 km. For the cloudy case the averaging kernels in the lower troposphere are generally more pronounced than those for the clear-sky situation. This higher sensitivity of the retrieval with respect to ozone in the lower model layers is due to the increase of light reflected in the troposphere by the presence of the cloud. However, using the CaA approach the averaging kernels in the troposphere peak at 1–3 km height, which is unrealistic since most light is reflected by the cloud top at 5 km altitude instead of by the surface. Using the $CUVO_2$ approaches, the peak of the tropospheric averaging kernels is located at the correct height, namely at the cloud top. Furthermore, the averaging kernels rapidly decrease below the cloud top as most of the

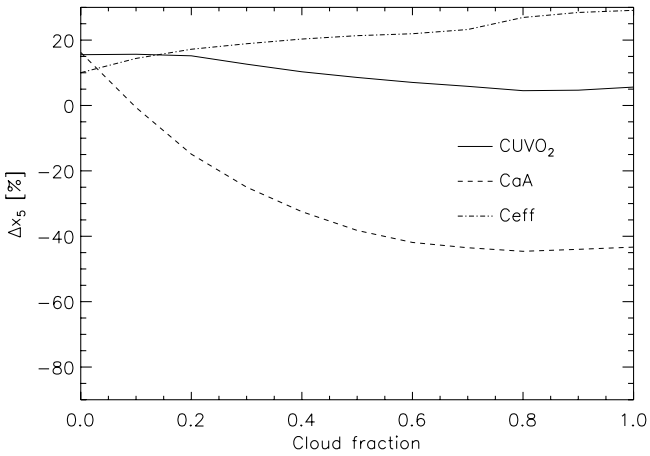

Figure 4. Similar to Figure 3a but when boundary-layer aerosols with a total optical thickness of 0.3 are included in the simulated measurements and the $CUVO_2$ (solid line), CaA (dashed lines), Ceff (dashed-dotted lines) approaches are used in the retrieval. Biomass burning aerosols corresponding type BH3 of *Torres et al.* [2001] are included in the bottom kilometer of the atmosphere. The two modes of these aerosols have an effective radius of respectively 0.145 μm and 3.28 μm and an effective size variance of respectively 0.174 and 0.704. The refractive index is $1.50 - 0.02i$. The fine mode fraction is 1.99×10^{-4}. See *Hansen and Travis* [1974] for the definitions of the parameters.

ozone in and below the cloud is effectively shielded. The averaging kernels for the Ceff approach are similar to those of the $CUVO_2$ approach.

[28] In conclusion of section 3, the CaA and Ceff approaches lead to significant biases in the mean tropospheric ozone concentrations, which increase with decreasing measurement and forward model errors. Furthermore, the underestimation due to the CaA approach increases with increasing cloud fraction, cloud optical thickness and cloud top height. The overestimation due to the Ceff approach generally increases with cloud fraction, decreases with cloud optical thickness but is relatively insensitive to the cloud top height. By using the $CUVO_2$ approach, these biases can be largely avoided. Furthermore, the averaging kernels in the troposphere obtained with the $CUVO_2$ and Ceff approaches peak at the correct altitude at the cloud top, in contrast to those obtained with the CaA approach which erroneously peak near the surface.

4. Effects of Clouds on GOME Ozone Profile Retrievals

[29] In this section we perform ozone profile retrievals from GOME data and compare results using the $CUVO_2$ approach with those obtained with the CaA and Ceff approaches. The retrievals are validated with ozonesonde measurements from April 1996 until April 1998, taken from the WOUDC for the five locations listed in Table 1. The

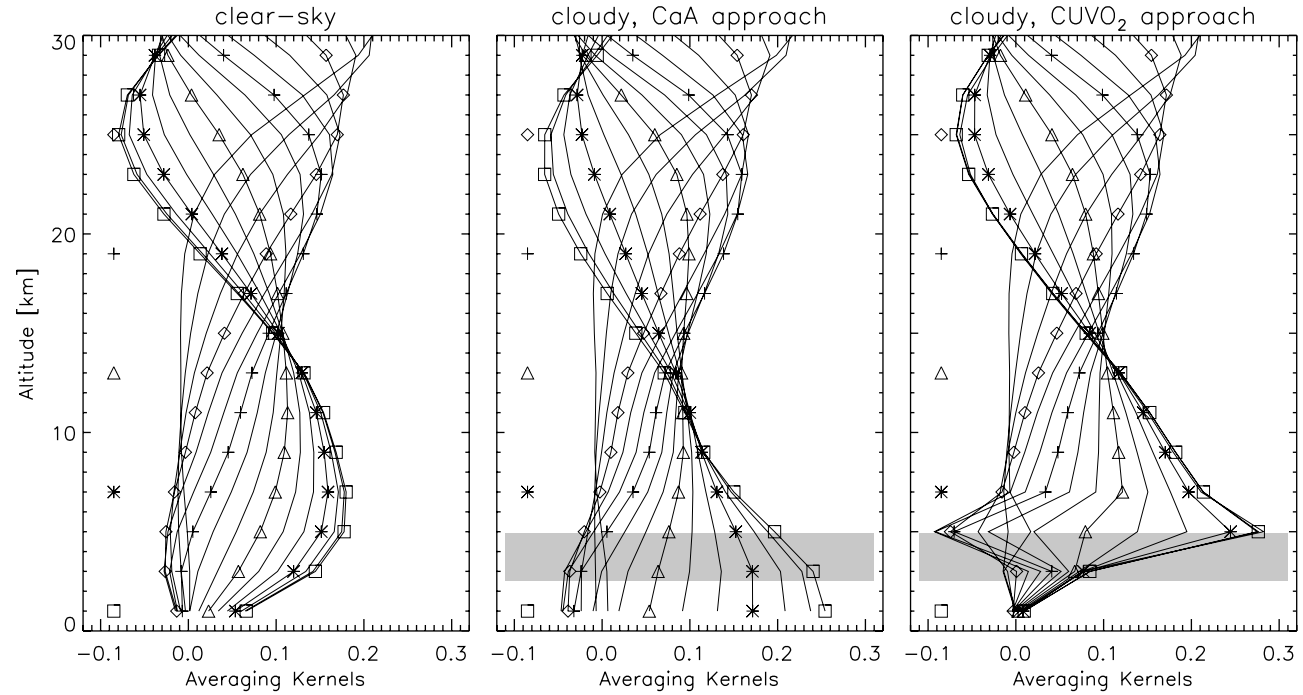

Figure 5. Three examples of averaging kernels for retrievals from simulated measurements of a clear-sky case (left panel) and a cloudy case, using the CaA approach (middle panel) and using the $CUVO_2$ or Ceff approach (right panel). The averaging kernels corresponding to atmospheric layers at 1, 7, 13, 19 and 25 km are indicated with squares, stars, triangles, pluses and diamonds, respectively. In the cloudy case, a cloud optical thickness of 10, a cloud top height of 5 km (520 hPa), a cloud base height of 2.8 km (720 hPa) and a cloud fraction of 1 is used. The grey area indicates the location of the cloud layer. A noise floor of 0.8% is used.

Table 1. Locations of Ozonesonde Stations Used for Validation

Station	Latitude	Longitude	Region	Colocations
Payerne	46.82	6.95	near alps	76
Hohenpeißenberg	47.80	11.02	near alps	65
Lauder	−45.03	169.683	New Zealand	50
Legionowo	52.4	20.967	near Berlin	20
Lindenberg	52.21	14.12	near Warsaw	22

sondes measure ozone concentrations up to a height of about 30 km with a precision of about 3–4% [*Beekmann et al.*, 1994]. The a priori surface albedos needed for the Ceff and $CUVO_2$ approaches are obtained from the database of *Koelemeijer et al.* [2003].

[30] Figure 6 shows a time series of the ozone densities x_5 at 5 km altitude retrieved using the $CUVO_2$ approach and the corresponding smoothed and unsmoothed ozonesonde measurements for the two stations near the alps, i.e. Payerne and Hohenpeißenberg. Figure 6 also shows the relative differences Δx_5 between x_5 retrieved using the $CUVO_2$, CaA and Ceff approaches and the corresponding smoothed sonde measurements, respectively. For the $CUVO_2$ approach, the comparison of the retrievals with the smoothed sonde measurement shows a good agreement, with Δx_5 distributed around 0. Δx_5 is somewhat larger in winter. On this scale the comparison for the Ceff approach appears similar to the $CUVO_2$ results. However, compared to the results from the $CUVO_2$ approach, Δx_5 obtained with the Ceff approach is more biased towards positive values in the winter months. Furthermore, a overall bias is present in the results of the Ceff approach which cannot be seen on this scale but will be shown below. In the results for the CaA approach a clear systematic bias of about 50% towards too low ozone concentrations can be seen. This is consistent with the results of *Hasekamp et al.* [2002] (Note that their Δx is reversed in sign), showing a similar time series for Payerne using the CaA approach. Similar results are obtained for the other three stations listed in Table 1.

[31] The differences between the results obtained with the CaA, Ceff and $CUVO_2$ approaches become more apparent in Figure 7, which shows the mean differences $\langle \Delta \mathbf{x} \rangle$ between the retrieved ozone profiles and the corresponding smoothed sonde measurements. The results are divided in two ranges in cloud optical thickness τ_c as retrieved by the $CUVO_2$ approach, namely $\tau_c > 40$ and $\tau_c < 40$. The results for $\tau_c < 40$ are very similar to the simulations shown in Figure 2. For $\tau_c > 40$, however, the Ceff and $CUVO_2$ approaches lead to unexpected large overestimations in the tropospheric ozone concentrations of about 40% at the surface. For about 38% of the measurements a cloud optical thickness above 40 is retrieved, which is much more often than expected (see e.g. *Chang and Li* [2005] who show a distribution of global optical thickness for different cloud types based on MODIS results). As we concluded previously [*van Diedenhoven et al.*, 2007] from comparison to ATSR-2 cloud retrievals, for the majority of such cases the

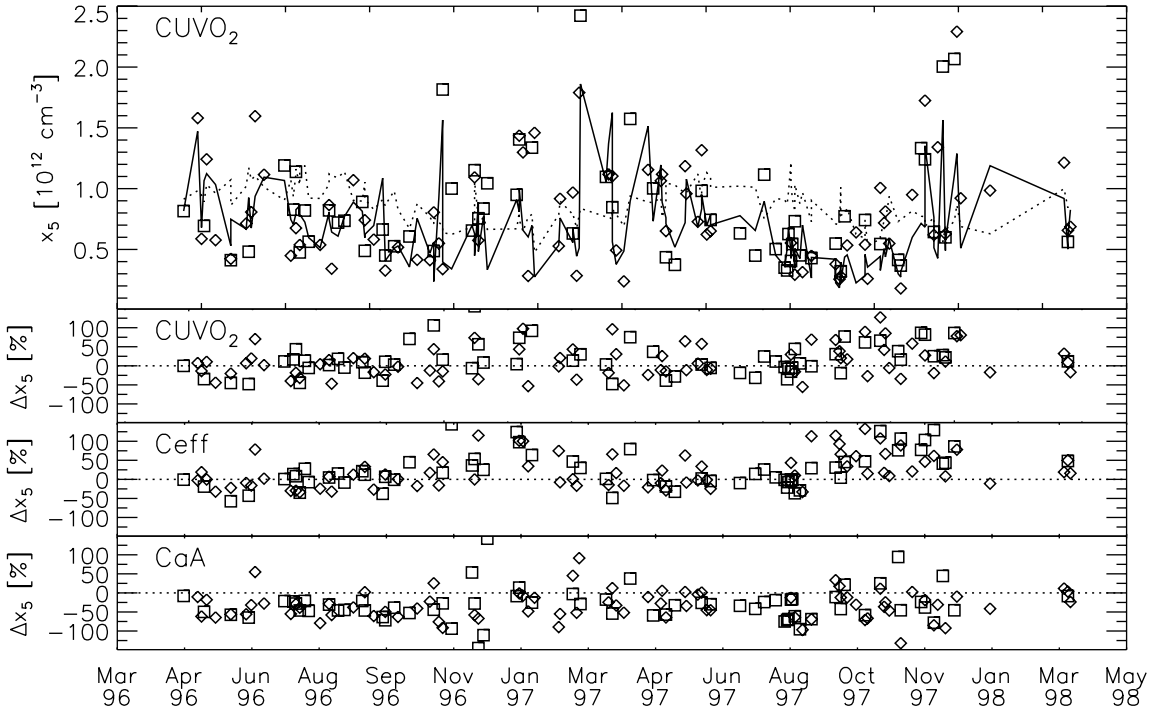

Figure 6. Time series of 141 GOME ozone profile retrievals at Payerne (diamonds) and Hohenpeißenberg (squares). The upper panel shows the absolute concentrations x_5 at 5 km altitude retrieved using the $CUVO_2$ approach and the corresponding ozonesonde measurements, smoothed by the retrieval averaging kernels (solid lines) and unsmoothed (dotted line). The bottom three panels show the relative differences Δx_5 between the retrievals and the smoothed sonde measurements for the $CUVO_2$, Ceff and CaA approaches, respectively. Here, Δx_5 is defined relative to the smoothed sonde values using the $CUVO_2$ averaging kernels.

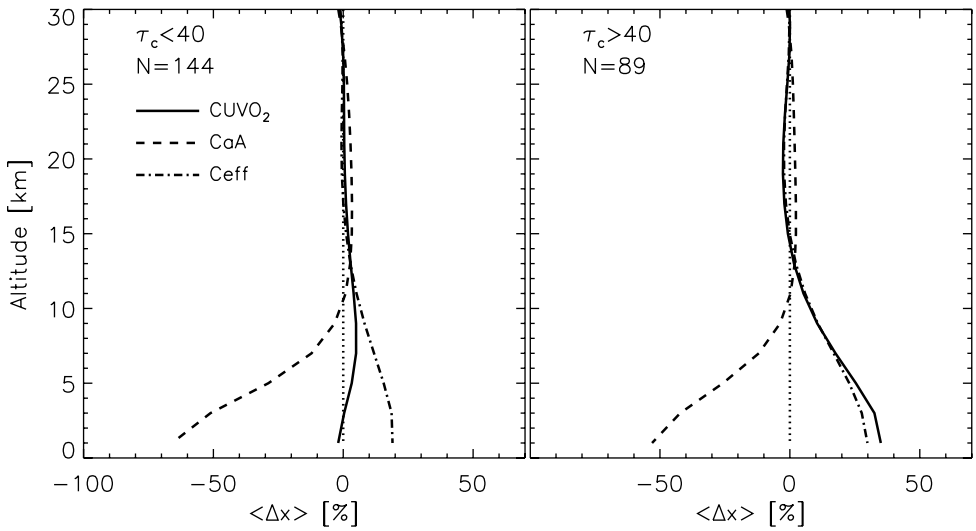

Figure 7. Relative average differences $\langle \Delta \mathbf{x} \rangle$ between the 233 GOME ozone profile retrievals and the corresponding smoothed ozone sonde measurements, for retrieved cloud optical thickness values τ_c below 40 (left) and above 40 (right). GOME retrievals are performed using the $CUVO_2$ (solid lines), CaA (dashed lines) and Ceff (dashed-dotted lines) approaches. The number of comparisons in each optical thickness range is indicated. Here, $\langle \Delta \mathbf{x} \rangle$ is defined relative to the mean smoothed sonde ozone profiles using the $CUVO_2$ averaging kernels.

retrieved cloud optical thickness is significantly overestimated while the cloud fraction is underestimated. These cases are related to the presence of horizontally inhomogeneous or multi-layered cloud fields. Obviously, the $CUVO_2$ and Ceff approaches are not adequate in the case of inhomogeneous clouds due to the assumption of a single homogeneous cloud layer and the independent pixel approximation. Therefore, we leave the case with $\tau_c > 40$ out of the further discussion.

[32] Figure 8 shows $\langle \Delta \mathbf{x} \rangle$ at the individual stations listed in Table 1 for $\tau < 5$ and $5 < \tau_c < 40$. For nearly all cases, the CaA approach leads to a similar underestimation of the mean ozone concentrations in the troposphere as obtained in the simulations of Figure 2. For $5 < \tau < 40$ this underestimation is up to about 80% near the surface and generally is significantly lower for $\tau < 5$, as expected from the results shown in Figure 3b. Only for the cases at Legionowo with $\tau < 5$ no underestimation is observed, which can be explained by the low cloud fraction (0.2 on average) observed here. However, the statistical value of the comparison is poor for this case.

[33] The $CUVO_2$ and Ceff approaches clearly improve the retrievals in the troposphere. For cloud optical thickness values below 5, the $CUVO_2$ approach leads to low errors of about ±10% for most stations. The Ceff approach leads to similar errors for these cloud optical thicknesses. Apparently, the positive and negative errors shown in Figure 3b for $\tau_c < 3$ and $3 < \tau_c < 5$, respectively, cancel each other. At Lindenberg, both $CUVO_2$ and Ceff approaches lead to unexpected overestimations of about 50% for $\tau_c < 5$.

[34] For cloud optical thickness values between 5 and 40, the $CUVO_2$ approach leads to errors below 10% for most stations, while the Ceff approach leads to an overestimation of about 25% in the lowest atmospheric layer, as expected from the simulations shown in Figure 2. At Lauder the Ceff approach leads to large relative errors up to 70%. The $CUVO_2$ approach shows an unexpected overestimation of about 20% in the lowest layer at Legionowo.

[35] The standard deviations $\boldsymbol{\sigma}_{\Delta x}$ of all 233 comparisons for the $CUVO_2$, CaA and Ceff approaches are shown in Figure 9. Similar results are obtained for the individual stations. For tropospheric layers, the standard deviation is about 75% near the surface, which is significantly larger than the 25% expected from the study on simulated measurements shown in Figure 2. Furthermore, $CUVO_2$ and Ceff approaches do not yield lower standard deviations than the CaA approach as expected from Figure 2. Also, no significant dependence of $\boldsymbol{\sigma}_{\Delta x}$ on retrieved cloud parameters is observed. This insensitivity to cloud parameters indicates that the large standard deviations are due to other causes than clouds. At least part of the large standard deviations is very likely due to GOME sub-pixel ozone variability; the sonde and GOME measurements do not measure the exact same air masses. *Sparling et al.* [2006] showed that the horizontal variability of middle and upper tropospheric ozone concentrations is 15–25% across scales of about 150 to 250 km. Even larger variabilities may be expected within the 960×80 km^2 footprints of GOME. Furthermore, due to the relatively broad averaging kernels in the troposphere (see Figures 5 and 4), the retrieved ozone values in the troposphere are significantly influenced by ozone concentrations in the lower stratosphere, where spatial variations can be large. However, the origin of the large standard deviations is an important issue to be looked further into in future work.

5. Conclusions

[36] In this paper we have evaluated a new approach to take clouds into account in ozone profile retrievals obtained from GOME measurements in the spectral range 290–340 nm. In this approach, ozone profile retrievals are performed using

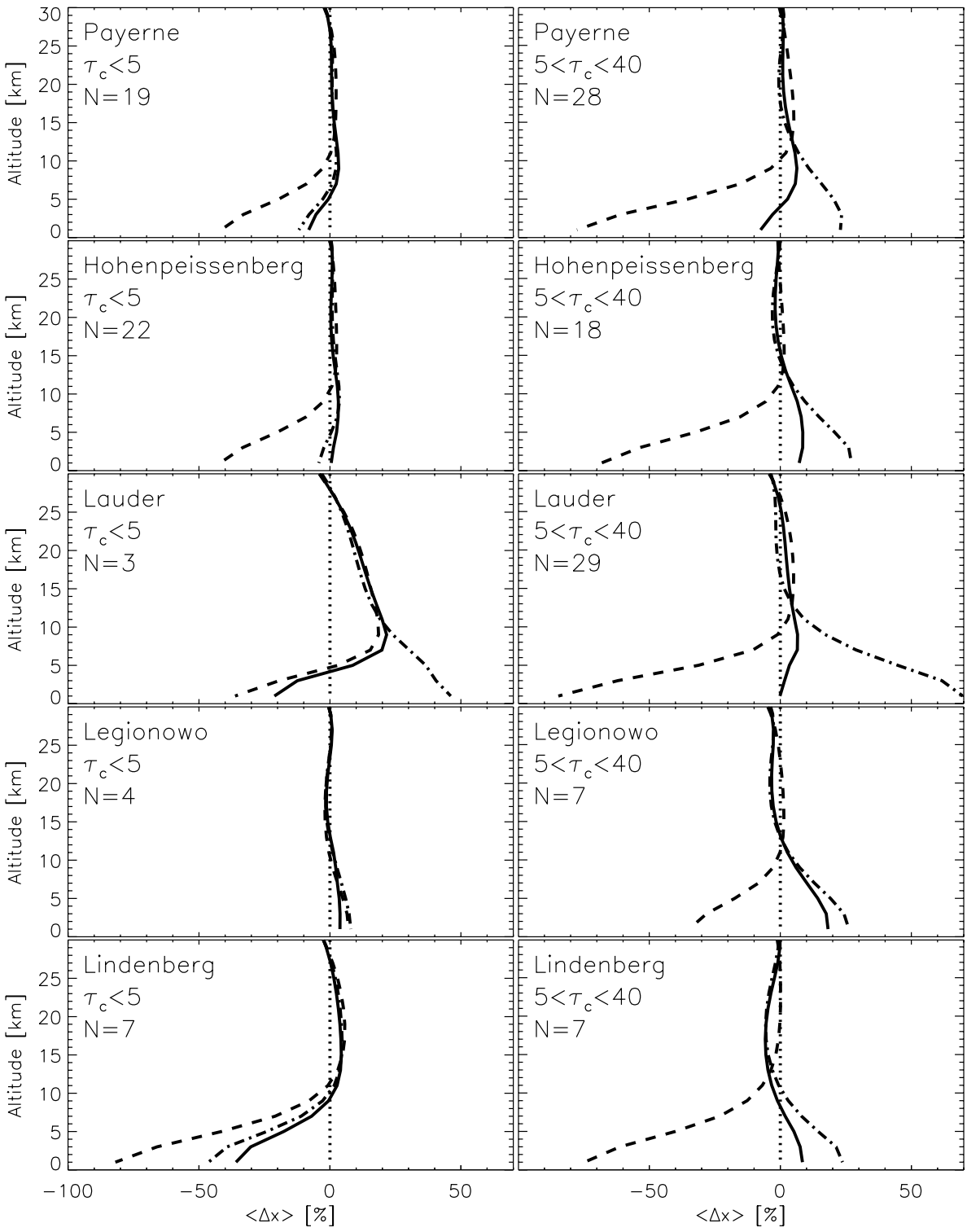

Figure 8. Similar to Figure 7 but for the 5 stations individually and for τ_c below 5 (left) and τ_c between 5 and 40 (right).

cloud fraction, cloud optical thickness and top pressure retrieved from oxygen A-band measurements combined with measurements in the range 350–390 nm [*van Diedenhoven et al.*, 2007]. This approach ($CUVO_2$) was compared with two commonly used approaches in ozone retrievals, namely (1) to treat clouds as an effective ground surface albedo (CaA approach); and (2) using effective cloud fractions and cloud top pressures retrieved from oxygen A-band measurements assuming a cloud optical thickness of 40 (Ceff approach). By means of simulated GOME retrievals for an ensemble of cases with varying cloud parameters we showed that the mean ozone concen-

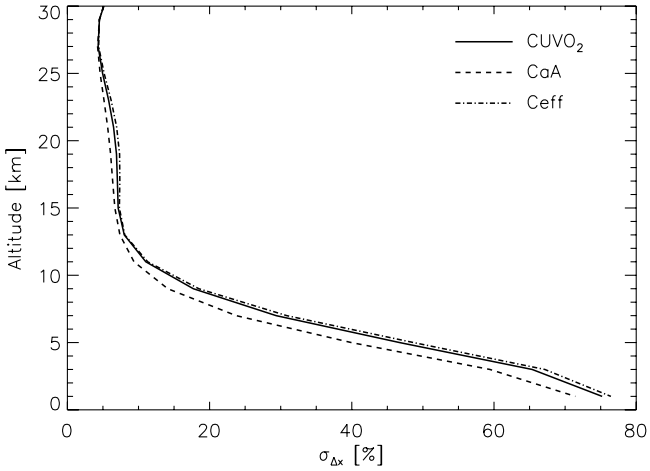

Figure 9. Relative standard deviation $\sigma_{\Delta x}$ of the differences between the 233 GOME ozone profiles retrieved using the $CUVO_2$ (solid line), CaA (dashed line) and Ceff (dashed-dotted line) approaches and the corresponding smoothed ozonesonde measurements.

trations are generally underestimated by up to 85% when using the CaA approach, while they are overestimated by up to 18% with the Ceff approach. The $CUVO_2$ approach leads to a relatively small underestimation of less than 3%. The errors generally peak near the surface. The underestimation due to the CaA approach is caused by the neglect of the fractional cloud cover and the elevation of clouds. The Ceff approach causes an overestimation due to the fact that the effective cloud fraction is a wavelength dependent quantity [*van Diedenhoven et al.*, 2007], and thus cannot be described by a single value. The presence of biomass-burning aerosols in the boundary layer with an optical thickness of 0.3 decreases the errors in tropospheric ozone obtained with the CaA approach by about 20% due to compensating errors. For the $CUVO_2$ and Ceff approaches, aerosols cause a positive (additional) bias of 5–15%, compared to the case without aerosols. It was shown that the obtained biases caused by the CaA and Ceff approach significantly increase with decreasing measurement and forward model errors. This is because a decrease of these errors leads to an increase in the contribution of tropospheric layers to the DFS.

[37] The three different approaches were then applied to ozone profile retrievals from 233 GOME measurements and the results were validated with co-located ozonesonde measurements at five different locations. For cases for which a cloud optical thickness above 40 is retrieved, it was shown that the $CUVO_2$ and Ceff approaches yield unexpected large overestimations of the tropospheric ozone concentrations of about 45%. There are indications that these cases are related to the presence of horizontally inhomogeneous or multi-layered cloud fields, where the cloud optical thickness is systematically overestimated [*van Diedenhoven et al.*, 2007]. Thus, the $CUVO_2$ and Ceff approaches are not adequate in the case of inhomogeneous clouds. The CaA approach leads to underestimations of about 70% for these cases. Also for the cases with $5 < \tau_c < 40$, the CaA approach generally leads to an underestimation of the mean ozone concentrations in the troposphere up to about 80%. As expected, smaller underestimations of about 40% are obtained with the CaA approach for optically thinner clouds. The Ceff approach leads to errors below 10% for $\tau_c < 5$, but shows overestimations of about 30% in the mean ozone concentrations near the surface for $5 < \tau_c < 40$, which is in accordance with the simulations. The $CUVO_2$ approach clearly improves on this and yields errors below 10% at most locations for all optical thicknesses below 40.

[38] The standard deviations of the differences between GOME retrievals and sonde measurements are generally up to about 75% near the surface, which is about 30–50% higher than those obtained in the simulations. The standard deviations are similar for all three approaches and are not dependent on cloud parameters. This indicates that these large standard deviations are not caused by clouds. At least part of these large standard deviations are very likely caused by the different airmasses probed by GOME and the ozonsondes [*Sparling et al.*, 2006]. However, the origin of the large standard deviations should be further investigated in future work.

[39] Overall, the CaA approach leads to significant underestimations in the mean tropospheric ozone concentrations retrieved from GOME measurements. The Ceff approach improves this but still leads to significant overestimations in the mean tropospheric ozone concentrations. For most cases, these errors can be largely avoided by using the $CUVO_2$ approach. The sensitivity of ozone profile retrievals to tropospheric layers can be increased by reducing forward model errors. Then, the biases due to the CaA and Ceff approaches significantly increase and the use of the $CUVO_2$ approach becomes even more relevant.

[40] **Acknowledgments.** The TOGOMI total ozone column data are obtained from the Tropospheric Emission Monitoring Internet Service (TEMIS) website (http://www.temis.nl). ESA is acknowledged for providing GOME data processed by DFD/DLR.

References

Beekmann, M., G. Ancellet, G. Mégie, H. G. J. Smit, and D. Kley (1994), Intercomparison campaign of vertical ozone profiles including electrochemical sondes of ECC and Brewer-Mast type and a ground based UV-differential absorption lidar, *J. Atm. Chem.*, *19*, 259–288.

Burrows, J. P., et al. (1999), The Global Ozone Monitoring Experiment (GOME): Mission concept and first scientific results, *J. Atmos. Sci.*, *56*, 151–175.

Chance, K., T. P. Kurosu, and C. E. Sioris (2005), Undersampling correction for array detector-based satellite spectrometers, *Appl. Opt.*, *44*, 1296–1304.

Chance, K. V., J. P. Burrows, D. Perner, and W. Schneider (1997), Satellite measurements of atmospheric ozone profiles, including tropospheric ozone, from UV/visible measurements in the nadir geometry: A potential method to retrieve tropospheric Ozone, *J. Quant. Spectrosc. Radiat. Transfer*, *57*, 476.

Chandra, S., J. R. Ziemke, and R. W. Stewart (1999), An 11-year solar cycle in tropospheric ozone from TOMS measurements, *Geophys. Res. Lett.*, *26*(2), 185–188.

Chang, F.-L., and Z. Li (2005), A near-global climatology of single-layer and overlapped clouds and their optical properties retrieved from Terra/MODIS data using a new algorithm, *J. Clim.*, *18*, 4752–4771.

de Laat, A. T. J., J. Landgraf, I. Aben, O. Hasekamp, and B. Bregman (2007), Validation of Global Ozone Monitoring Experiment ozone profiles and evaluation of stratospheric transport in a global chemistry-transport model, *J. Geophys. Res.*, *112*, D05301, doi:10.1029/2005JD006789.

DLR (2002), GOME Data Processor - Extraction Software User's Manual, *DLR Report, ER-SUM-DLR-GO-0045, Issue 2*.

Hansen, J. E., and L. D. Travis (1974), Light scattering in planetary atmospheres, *Sp. Sci. Rev.*, *16*, 527–610.

Hansen, P., and D. O'Leary (1993), The use of the L-curve in the regularization of discrete ill posed problems, *SIAM J. Sci. Comput.*, *14*, 1487–1503.

Hasekamp, O. P., and J. Landgraf (2001), Ozone profile retrieval from backscattered ultraviolet radiances: The inverse problem solved by regularization, *J. Geophys. Res.*, *106*(D8), 8077–8088.

Hasekamp, O. P., and J. Landgraf (2002), A linearized vector radiative transfer model for atmospheric trace gas retrieval, *J. Quant. Spectrosc. Radiat. Transfer*, *75*, 221–238.

Hasekamp, O. P., and J. Landgraf (2005), Linearization of vector radiative transfer with respect to aerosol properties and its use in satellite remote sensing, *J. Geophys. Res.*, *110*, D04203, doi:10.1029/2004JD005260.

Hasekamp, O. P., J. Landgraf, and R. van Oss (2002), The need of polarization modeling for ozone profile retrieval from backscattered sunlight, *J. Geophys. Res.*, *107*(D23), 4692, doi:10.1029/2002JD002387.

Hoogen, R., V. V. Rozanov, and J. P. Burrows (1999), Ozone profiles from GOME satellite data: Algorithm description and first validation, *J. Geophys. Res.*, *104*(D7), 8263–8280.

Koelemeijer, R. B. A., and P. Stammes (1999), Effects of clouds on ozone column retrieval from GOME UV measurements, *J. Geophys. Res.*, *104*(D7), 8281–8294.

Koelemeijer, R. B. A., P. Stammes, J. W. Hovenier, and J. F. de Haan (2001), A fast method for retrieval of cloud parameters using Oxygen A band measurements from the Global Ozone Monitoring Experiment, *J. Geophys. Res.*, *106*(D4), 3475–3490.

Koelemeijer, R. B. A., J. F. de Haan, and P. Stammes (2003), A database of spectral surface reflectivity in the range 335–772 nm derived from 5.5 years of GOME observations, *J. Geophys. Res.*, *108*(D2), 4070, doi:10.1029/2002JD002429.

Krijger, J., I. Aben, and J. Landgraf (2005), *CHEOPS-GOME: WP2.1: Study of Instrument Degradation*, ESA SRON-EOS/RP/05-018 Tech. rep.

Krijger, J., M. van Weele, I. Aben, and R. Frey (2007), Technical Note: The effect of sensor resolution on the number of cloud-free observations from space, *Atm. Chem. Phys.*, *7*, 2881–2891.

Landgraf, J., and O. P. Hasekamp (2007), Retrieval of tropospheric ozone: The synergistic use of thermal infrared emission and ultraviolet reflectivity measurements from space, *J. Geophys. Res.*, *112*, D08310, doi:10.1029/2006JD008097.

Landgraf, J., O. P. Hasekamp, M. A. Box, and T. Trautmann (2001), A linearized radiative transfer model for ozone profile retrieval using the analytical forward-adjoint perturbation theory approach, *J. Geophys. Res.*, *106*(D21), 27,291–27,306.

Landgraf, J., O. P. Hasekamp, and T. Trautmann (2002), Linearization of radiative transfer with respect to surface properties, *J. Quant. Spectrosc. Radiat. Transfer*, *72*, 327–339.

Landgraf, J., O. P. Hasekamp, R. van Deelen, and I. Aben (2004), Rotational Raman scattering of polarized light in the Earth atmosphere: A vector radiative transfer model using the radiative transfer perturbation theory approach, *J. Quant. Spectrosc. Radiat. Transfer*, *87*, 399–433.

Liu, X., K. Chance, C. E. Sioris, R. J. D. Spurr, T. P. Kurosu, R. V. Martin, and M. J. Newchurch (2005), Ozone profile and tropospheric ozone retrievals from the Global Ozone Monitoring Experiment: Algorithm description and validation, *J. Geophys. Res.*, *110*, D20307, doi:10.1029/2005JD006240.

Liu, X., K. Chance, and T. P. Kurosu (2007a), Improved ozone profile retrievals from GOME data with degradation correction in reflectance, *Atm. Chem. Phys.*, *7*, 1575–1583.

Liu, X., K. Chance, C. E. Sioris, and T. P. Kurosu (2007b), Impact of using different ozone cross sections on ozone profile retrievals from Global Ozone Monitoring Experiment (GOME) ultraviolet measurements, *Atm. Chem. Phys.*, *7*, 3571–3578.

Marshak, A., A. Davis, W. Wiscombe, and G. Titov (1995), The verisimilitude of the independent pixel approximation used in cloud remote sensing, *Remote Sens. Environ.*, *52*, 71–78.

Meijer, Y. J., et al. (2006), Evaluation of Global Ozone Monitoring Experiment (GOME) ozone profiles from nine different algorithms, *J. Geophys. Res.*, *111*, D21306, doi:10.1029/2005JD006778.

Munro, R., R. Siddans, W. J. Reburn, and B. J. Kerridge (1998), Direct measurements of tropospheric ozone from space, *Nature*, *392*, 168–171.

Orphal, J. (2003), A critical review of the absorption cross-sections of O_3 and NO_2 in the ultraviolet and visible, *J. Photochem. and Photobiol. A*, *157*, 185–209.

Phillips, P. (1962), A technique for the numerical solution of certain integral equations of the first kind, *J. Assoc. Comput. Mach.*, *9*, 84–97.

Rodgers, C. (2000), *Inverse Methods for Atmospheric Sounding: Theory and Practice*, World Sc., River Edge, N. J.

Rossow, W. B., and A. A. Lacis (1990), Global, seasonal cloud variations from satellite radiance measurements. part II. Cloud properties and radiative effects, *J. Clim.*, *3*, 1204–1253.

Slijkhuis, S. (2004), CHEOPS-GOME: Study on seasonal effects on the ERS-2/GOME diffuser BSDF, *DLR Report, Doc. No.: CH-TN-DLR-GO-0001*.

Sparling, L. C., J. C. Wei, and L. M. Avallone (2006), Estimating the impact of small-scale variability in satellite measurement validation, *J. Geophys. Res.*, *111*, D20310, doi:10.1029/2005JD006943.

Tikhonov, A. (1963), On the solution of incorrectly stated problems and a method of regularization, *Dokl. Akad. Nauk SSSR*, *151*, 501–504.

Torres, O., R. Decea, P. Veefkind, and G. de Leeuw (2001), Omi aerosol retrieval algorithm, *ATBD-OMI-03*.

Valks, P., and R. van Oss (2003), TOGOMI Algorithm Theoretical Basis Document, Issue 1.2, *TOGOMI/KNMI/ATBD/001, KNMI/ESA*.

van Deelen, R., O. P. Hasekamp, and J. Landgraf (2007), Accurate modeling of spectral fine-structure in Earth radiance spectra measured with the Global Ozone Monitoring Experiment, *Appl. Opt.*, *46*, 243–252.

van der A, R. J., R. F. van Oss, A. J. M. Piters, J. P. F. Fortuin, Y. J. Meijer, and H. M. Kelder (2002), Ozone profile retrieval from recalibrated Global Ozone Monitoring Experiment data, *J. Geophys. Res.*, *107*(D15), 4239, doi:10.1029/2001JD000696.

van Diedenhoven, B., O. P. Hasekamp, and J. Landgraf (2006), Efficient vector radiative transfer calculations in vertically inhomogeneous cloudy atmospheres, *Appl. Opt.*, *45*, 5993–6006.

van Diedenhoven, B., O. P. Hasekamp, and J. Landgraf (2007), Retrieval of cloud parameters from satellite-based reflectance measurements in the ultraviolet and the oxygen A-band, *J. Geophys. Res.*, *112*, D15208, doi:10.1029/2006JD008155.

van Oss, R. F., R. H. M. Voors, and R. J. D. Spurr (2002), Ozone profile algorithm, in *OMI Algorithm Theoretical Basis Document, Volume II: OMI Ozone Products*, edited by P. K. Bhartia, pp. 51–73.

Voigt, S., J. Orphal, K. Bogumil, and J. Burrows (2001), The temperature dependence (203–293 K) of the absorption cross sections of O_3 in the 230–850 nm region measured by Fourier-transform spectroscopy, *J. Photochem. Photobiol. A: Chem.*, *143*, 1–9.

Wang, P., P. Stammes, and F. Boersma (2006), Impact of the effective cloud fraction assumption on tropospheric NO_2 retrievals, in *Proceedings of the First Atmospheric Science Conference, Frascati, Italy (ESA SP-628)*.

Ziemke, J. R., S. Chandra, and P. K. Bhartia (2005), A 25-year data record of atmospheric ozone in the Pacific from Total Ozone Mapping Spectrometer (TOMS) cloud slicing: Implications for ozone trends in the stratosphere and troposphere, *J. Geophys. Res.*, *110*, D15105, doi:10.1029/2004JD005687.

O. P. Hasekamp and J. Landgraf, SRON Netherlands Institute for Space Research, Earth Oriented Science Division, Sorbonnelaan 2, 3584 CA Utrecht, Netherlands.

B. van Diedenhoven, NASA Goddard Institute for Space Studies, 2880 Broadway, New York, NY 10025, USA. (bvandiedenhoven@giss.nasa.gov)